JJC

Volume 17, Number 1, 2022
Pages 1–12

Jordan Journal of Chemistry
https://doi.org/10.47014/17.1.1

ARTICLE

Optimization of *p*-Nitroaniline Adsorption from Aqueous Medium by TiO_2-Flamboyant Seeds Activated Carbon Composite

Samsudeen Olanrewaju Azeez[a]*, Akeem Adebayo Jimoh[a], Ismaila Olalekan Saheed[a], Damilola Tope Ogundele[a], Folahan Amoo Adekola[b], Zuliah Abiola Abdulsalam[a] and Kuranga Ibrahim Ayinla[b]

[a] *Kwara State University, Faculty of Pure and Applied Sciences, Department of Chemistry and Industrial Chemistry, 241103, Malete, Nigeria.*
[b] *University of Ilorin, Faculty of Physical Sciences, Department of Industrial Chemistry, 240003, Ilorin, Nigeria.*

Received: 29th Nov. 2021; *Accepted:1st March 2022*

Abstract: Titanium (IV) oxide-flamboyant seeds activated carbon (TiO_2-FSAC) composite was studied as a promising adsorbent for *p*-nitroaniline (*p*-NA) removal from aqueous media using batch technique. The surface characteristics of the composite were determined by Fourier Transform Infrared Spectroscopy, Scanning Electron Microscopy, Energy Dispersed X-ray Spectroscopy and Brunauer–Emmett–Teller surface area analysis. The results showed that TiO_2-FSAC is highly porous with a surface area of 601.77 m^2/g and pore diameter in the mesoporous region. Box-Behnken design (BBD) under Response Surface Methodology (RSM) was employed for the optimization of four operating parameters: initial *p*-NA concentration, pH, adsorbent dosage and time. The results revealed that the amount of *p*-NA adsorbed increased with an increase in initial *p*-NA concentration, low pH, and low adsorbent dosage and was not affected by time in the investigated range. The correlation between *p*-NA adsorption by TiO_2-FSAC and the process variables was sufficiently established by the quadratic model with a high R^2 value (0.973), which is in agreement with adjusted R^2 (0.945). The optimum amount of *p*-NA adsorbed was 45.0 mg/g accomplished at C_o = 300 mg/L, pH 2, 0.1 g adsorbent dosage and 362.5 min time.

Keywords: Adsorption, Box-Behnken design, *p*-nitroaniline, Flamboyant seed activated carbon, Titanium(IV) oxide, ANOVA.

Introduction

In developing countries, water pollution caused by organic contaminants, like *p*-nitroaniline (*p*-NA), is of great concern[1]. *p*-NA is a highly toxic compound used, among others, as a precursor in the production of dyes, *p*-phenylenediamine, antioxidants, pesticides and pharmaceutical synthesis[2]. The discharge of *p*-NA directly into the eco-system, even at lower concentrations, will negatively impact the environment as a result of its carcinogenic, mutagenic and toxic effects[2,3]. Hence, the removal of *p*-NA from wastewater is of great importance, and environment-friendly, cost-effective methods must be developed for its removal.

In the past, some biological, chemical and physical techniques have been employed for the adsorption of *p*-NA and other organics from aqueous solutions. Along with that, these techniques are not environment-friendly, they are expensive, inefficient and generate toxic secondary products[2,4]. Adsorption has been regarded as one of the most encouraging technologies in the removal of *p*-NA. Low-cost

*Corresponding Author: Samsudeen Olanrewaju Azeez **Email**: samsudeen.azeez@kwasu.edu.ng

materials from agricultural wastes for the removal of organic pollutants in wastewater are gaining acceptance from scientists[4–6]. Now, new materials that are highly effective and cheap to treat wastewater are being sought and developed by researchers[4,5,7–9].

To dig into the utilization of abundant and cheap adsorbents, activated carbon from agricultural wastes blended with metal oxides, like TiO_2, is considered for the removal of organic pollutants from wastewater. TiO_2 is a non-toxic cheap semiconductor. As a result of its high stability and potential in degrading organic pollutants in aqueous media, it is the most used photocatalyst[10]. It produces electron-hole pairs that allow chemical modification of the reacting species. Blending TiO_2 with activated carbon as a support has also been investigated[11,12]. The hydroxyl groups (–OH) on the surface of activated carbon attract the pollutants towards the surface of the photocatalyst and increase thus the interaction probability with TiO_2. The combined effect of the TiO_2-activated carbon composite, therefore, enhances the total efficiency of the adsorption process[11].

Flamboyant, also named Royal Poinciana, is called Pansheke in the Yoruba language in Nigeria. The seeds are non-edible and are considered as agricultural wastes[13].

The optimization of adsorption parameters is most frequently studied by varying one parameter while keeping the others constant. But, this approach does not reflect the interactive effects of all parameters[14]. This technique wastes time, requires a lot of experiments and uses large amounts of chemicals. These disadvantages can be overcome by optimizing the variables simultaneously using a statistical experimental design, such as the Box-Behnken design (BBD) in response surface methodology (RSM)[15,16].

This research work intended to optimize the adsorption of *p*-NA from aqueous media using TiO_2-flamboyant seeds-activated carbon composite.

Materials and Methods

Adsorbent Preparation and Characterization

The flamboyant seeds used were washed and sun-dried. The seeds were carbonized in a muffle furnace (Carbolite CWF 1300) at 450 °C for 120 min. After pulverizing and sieving (standard mesh < 63 µm), an amount of 100 g of the carbonized flamboyant seed was impregnated in 500 mL of 1.0 M nitric acid for 48 h and afterward, filtered, washed to neutral pH and dried at 110 °C. It was then ground and sieved into < 63 µm and labeled flamboyant seeds-activated carbon (FSAC)[1].

TiO_2-FSAC was obtained by adding 10 g of FSAC to 100 mL of deionized water. It was vigorously mixed for 1 h, then an amount of 5 g of commercial TiO_2 nanoparticles was added and agitated for 2 h at 40 °C[17]. The suspension was decanted and a 1:1 ratio of ethanol and water solution was added to the resulting TiO_2-FSAC, which was then hydrothermally treated in an autoclave at 120 °C for 2 h. The composite was centrifuged at 4000 rpm for 15 min, washed and oven-dried at 110 °C for 1 h. It was then calcined at 400 °C for 3 h. After cooling, it was ground into fine particles and stored for further use[17,18]. The prepared TiO_2-FSAC was characterized by FTIR (Perkin-Elmer Spectrum GX- FTIR Spectrometer version 10.6 0, TU, Dublin), to determine the functional groups present. The surface morphologies and composition of the material were recorded with SEM (SEM/EDX ASPEX 3020 model Delmont, PA 15626-1723 – USA). The surface area was determined by BET analysis of N_2 adsorption using a BET surface area analyzer (Micromeritics ASAP 2020 V3.02H model, Norcross, GA, U.S.A).

Preparation of Adsorbate

A stock solution of *p*-NA was prepared by dissolving 1.00 g of *p*-NA in 50 mL ethanol and then filled to the mark with de-ionized water in a 1000-mL standard volumetric flask. Different working solutions were prepared from the stock solution by serial dilution[4,6].

Adsorption Experiment

The adsorption experiments were carried out using the batch method. 20 mL each of *p*-NA solutions of various concentrations (50–300 mg/L) were transferred to 100-mL conical flasks. The effect of various experimental parameters was investigated: pH (2.0–12.0), contact time (5–720 min) and adsorbent dosage (0.10–0.50 g/20 mL of TiO_2 -FSAC). A sample of 0.10 g of TiO_2-FSAC was added to each of the flasks and the pH was adjusted using 0.10 M NaOH or 0.10 M HCl solution. It was agitated at 200 rpm and 30 ± 2 °C. The samples were analyzed using a UV-Vis spectrophotometer (Microprocessor UV-VIS Double Beam AVI-2802) at λ_{max}= 400 nm[4].

The amount of *p*-NA adsorbed (q_e) was calculated using Equation 1:

$$q_e = \frac{(C_0 - C_e)V}{W} \quad (1)$$

where q_e is the amount of *p*-NA adsorbed per gram, C_o is the initial *p*-NA concentration (mg/L), C_e is the equilibrium *p*-NA concentration (mg/L), V is the volume of *p*-NA solution (L) and W is the weight of TiO_2 -FSAC (g).

Box-Behnken Experimental Design and Optimization Process

Box-Behnken experimental design (BBD) under response surface methodology (RSM) was applied to explain and validate the interaction between the adsorption parameters. The design was used to develop sets of designed experiments by Design Expert 11.1.2.0 with four factors; namely *p*-NA concentration (A), pH (B), adsorbent dosage (C) and contact time (D), investigated each at three levels. The experimental range and levels of the operating variables are given in Table 1. The matrix of Box-Behnken experimental design with the corresponding responses are tabulated in Table 2 and were examined statistically. The number of experimental runs in BBD could as well be calculated using Equation 2.

$$N = k^2 + k + C_p \quad (2)$$

where *N* is the number of experimental runs, *k* is the number of factors and C_p is the replicate number of the center points.

Table 1. Process variables and corresponding coded levels.

Operational variables	Levels		
	-1	**0**	**1**
Initial *p*-NA concentration (mg/g)	50	175	300
pH	2	7	12
Dosage (g/20 mL)	0.1	0.3	0.5
Time (min)	5	362.5	720

Consequently, a total of 29 experimental runs were carried out based on the four factors and three-level design with their coded values, (–1, 0, +1), as shown in Table 1 and Table 3. The experimental data were studied and found to fit the second-order polynomial model that gives an insight into the nature of the process as expressed by Equation 3.

$$R = \beta_0 + \sum_{i=1}^{k} \beta_i x_i + \sum_{i=1}^{k} \beta_{ii} x_i^2 + \sum_{1 \le i \le j}^{k} \beta_{ij} x_i x_j + \epsilon \quad (3)$$

R is, thereby, the response (amount of *p*-NA adsorbed per gram); x_i = variables; *k* = number of variables; β_0 = constant term; β_i = coefficients of linear parameters; β_{ij} = coefficient of the interaction parameters; β_{ii} = coefficient of the quadratic parameter; ε = residual associated to the experiments.

Results and Discussion

Characterization of FSAC-TiO2

The elemental composition of the adsorbent as determined by EDX is presented in Table 2. The major elements detected are Ti (33.38%), O (36.23%) and C (29.44%), affirming that TiO_2-FSAC was prepared.

Table 2. Characteristics of TiO_2-FSAC.

Parameters	Values
%C	29.44
%O	36.23
%Ti	33.38
%Ca	0.52
%K	0.43
BET Surface area (m^2g^{-1})	601.77
Average pore volume (cm^3g^{-1})	0.16
Average pore diameter (nm)	6.04

The SEM micrograph of FSAC-TiO_2 before adsorption (Figure 1a) showed that there are many pores available for adsorption of *p*-NA with uneven flaky-like agglomeration of fine particles due to activation by acid treatment and TiO_2 loaded on the carbon[11,19]. The SEM micrograph of TiO_2-FSAC after adsorption of *p*-NA (Figure 1b) revealed that the surface of the adsorbent undergoes textural changes upon adsorption. Also, the SEM image of bear FSAC before adsorption (Figure 1c) is presented for comparison.

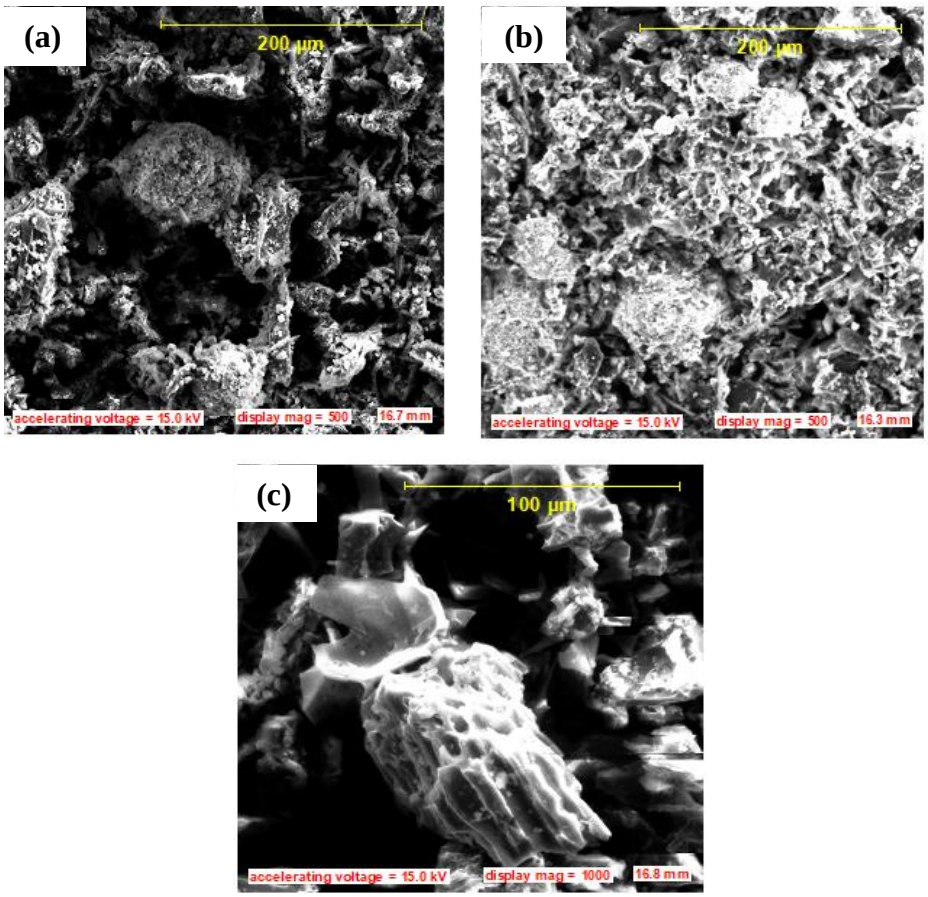


Figure 1. SEM images of TiO_2-FSAC: (a) before adsorption (b) after *p*-NA adsorption (c) FSAC.

The BET analysis results are presented in Table 2. The surface area of the adsorbent is large indicating that TiO_2-FSAC would be an excellent material in the uptake of *p*-NA. The table also shows that the pore diameter is high in the mesoporous range (2–50 nm)[4,11]. It is thus assumed that TiO_2-FSAC would be a good material for the removal of *p*-NA.

Figure 2 shows the FTIR spectra of TiO_2-FSAC and FSAC. It revealed distinct absorption bands which were identified at 3407 cm^{-1} due to the O-H stretching vibration of the phenolic, carboxylic and lactonic groups on the surface of the adsorbent, as well as water adsorbed from the atmosphere. The band at 1612 cm^{-1} corresponds to the aromatic C=C stretch, that at 1384 cm^{-1} is characteristic of the C-OH stretch, while that at 780 cm^{-1} is ascribed to the out-of-plane C-H bending vibration. The strong absorption below 600 cm^{-1} is attributed to the vibrations of TiO_2[4,5,20–22], which shows that TiO_2-FSAC was successfully prepared.

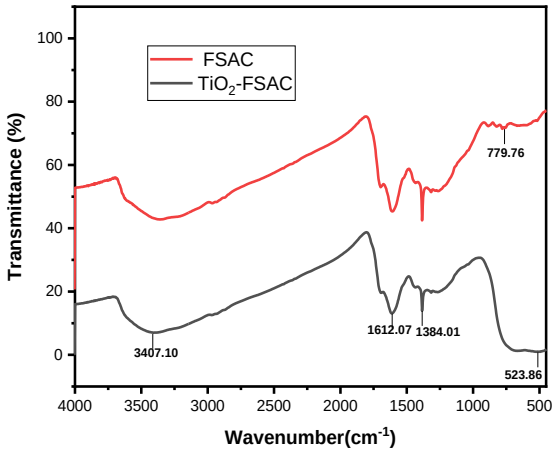


Figure 2. FTIR spectra of TiO_2-FSAC and FSAC.

Optimization of *p*-NA Adsorption onto TiO_2-FSAC by Box-Behnken Design (BBD)

Box–Behnken design in response surface methodology (RSM) was applied to ascertain the optimum conditions for adsorption of *p*-NA by TiO_2-FSAC. The complete design matrix of four process parameters, initial *p*-NA concentration, pH, adsorbent dosage and contact time, each at three levels with respect to actual and predicted responses (amount adsorbed per gram) are presented in Table 3.

Table 3. Box-Behnken experimental design for *p*-NA adsorption by TiO_2-FSAC.

Experimental run	Independent variables				Response (mg/g)	
	(A) Concentration (mg/L)	**(B)** pH	**(C)** Dosage (g/20 mL)	**(D)** Time (min)	Actual quantity adsorbed	Predicted quantity adsorbed
1	300	7	0.3	5	17.07	18.70
2	175	7	0.1	720	31.89	29.08
3	175	2	0.3	720	11.66	13.61
4	175	7	0.3	362.5	9.92	9.72
5	175	7	0.1	5	25.28	25.11
6	300	12	0.3	362.5	15.93	15.68
7	175	7	0.3	362.5	10.12	9.72
8	175	12	0.3	5	8.33	7.66
9	50	7	0.3	5	0.78	0.13
10	300	2	0.1	362.5	45.02	43.90
11	175	2	0.5	362.5	6.79	6.60
12	175	7	0.5	720	6.62	5.12
13	300	2	0.3	362.5	19.52	21.29
14	175	7	0.3	362.5	9.69	9.72
15	50	2	0.3	362.5	3.28	1.86
16	50	7	0.3	720	2.49	1.25
17	50	12	0.3	362.5	1.33	-2.10
18	300	7	0.3	720	18.85	19.89
19	175	12	0.1	362.5	22.38	22.96
20	175	12	0.5	362.5	2.45	3.66
21	300	7	0.5	362.5	10.58	7.52
22	175	2	0.1	362.5	30.42	29.60
23	50	7	0.1	362.5	5.72	10.06
24	175	12	0.3	720	3.59	6.15
25	50	7	0.5	362.5	1.74	4.14
26	175	2	0.3	5	11.05	9.77
27	175	7	0.5	5	5.62	6.76
28	175	7	0.3	362.5	9.13	9.72
29	175	7	0.3	362.5	9.72	9.72

The second-order quadratic model equation that relates the adsorption responses with the process variables was achieved by Design Expert 11.1.2.0 and is depicted by Equation 4. Also, the insignificant terms in Equation 4 with p values > 0.05 were taken out to affirm the statistically significant regression model. Hence, Equation 5 was achieved. Equations 4 and 5 revealed how the interactive model terms influenced the adsorption of *p*-NA from aqueous solution by TiO_2-FSAC.

$$Y = +9.72 + 9.30A - 2.39B - 10.58C + 0.5808D - 0.4100AB - 7.62AC + 0.0175AD + 0.9250BC - 1.34BD - 1.40CD + 0.0812A^2 - 0.6163B^2 + 6.61C^2 + 0.1962D^2 \quad (4)$$

$$Y = +9.72 + 9.30A - 2.39B - 10.58C + 0.5808D - 7.62AC + 6.61C^2 + 6.61 \quad (5)$$

ANOVA Results

The suitability of the statistical model was confirmed using the ANOVA test. The results obtained are tabulated in Table 4. The model F-value of 35.55 at a p-value of less than 0.05 implies that the second-order quadratic model is significant with a high regression coefficient (R^2) value of 0.973. The adjusted R^2 (0.945) is in good agreement with the predicted R^2 (0.843), since the difference is less than 0.2. This is indicative of the acceptability of the model tested. Also, the low value of the percentage coefficient of variation (CV%) 20.01% and 26.80% indicates good reliability and high precision of the experimental values[15]. The linear model terms (A, B, C), the interaction term AC and quadratic terms C^2 are statistically significant ($p < 0.05$). This is to say that the number of experiments carried out was sufficient to illustrate the influence of the operating variables on the amount of *p*-NA adsorbed from an aqueous solution[23–25].

Table 4. ANOVA analysis using BBD under RSM for *p*-NA adsorption onto TiO_2-FSAC.

Source	Sum of squares	df	Mean square	F-value	p-value	Comments	%C
Model	3019.03	14	215.65	35.55	< 0.0001	Significant	34.40
A-Conc	1038.44	1	1038.44	171.19	< 0.0001	Significant	2.28
B-pH	68.69	1	68.69	11.32	0.0046	Significant	44.46
C-Dosage	1342.18	1	1342.18	221.26	< 0.0001	Significant	0.13
D-Time	4.05	1	4.05	0.6674	0.4277		0.02
AB	0.6724	1	0.6724	0.1108	0.7441		7.68
AC	231.95	1	231.95	38.24	< 0.0001	Significant	0.00
AD	0.0012	1	0.0012	0.0002	0.9889		0.11
BC	3.42	1	3.42	0.5642	0.4650		0.24
BD	7.16	1	7.16	1.18	0.2958		0.26
CD	7.87	1	7.87	1.30	0.2739		0.001
A^2	0.0427	1	0.0427	0.0070	0.9343		0.081
B^2	2.46	1	2.46	0.4062	0.5342		9.38
C^2	283.08	1	283.08	46.67	< 0.0001	**S**ignificant	0.008
D^2	0.2496	1	0.2496	0.0411	0.8422		34.40
Residual	84.93	14	6.07				
Lack of fit	84.38	10	8.44	61.49			
Pure error	0.5489	4	0.1372				
Cor.total	3103.96	28					
Std. dev.	2.46						

Mean = 12.31; C.V.% = 20.01; R^2 = 0.973; Adjusted. R^2 = 0.945; Predicted. R^2 = 0.843; Adequate Precision = 25.970.

The plot of actual against predicted response values of *p*-NA removal onto TiO_2-FSAC is given in Figure 3. The points on the graph are well aligned on the straight line, inferring a good agreement between the actual and predicted values of the response. This suggests that the proposed statistical model is adequate for the optimization of *p*-NA removal by TiO_2-FSAC[26].

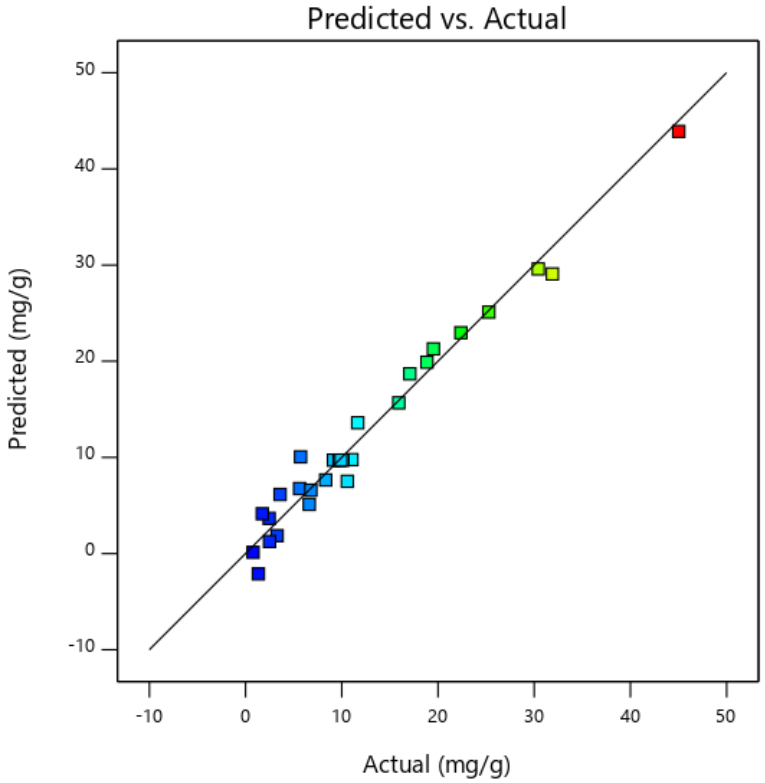


Figure 3. Correlation between actual and predicted responses for *p*-NA adsorption onto TiO_2-FSAC.

Effect of Process Parameters on the Adsorption of *p*-NA onto TiO_2-FSAC

The effect of the various operating parameters on the amount of *p*-NA adsorbed from aqueous solution by TiO_2-FSAC is depicted by 3D response surface plots (Figures 4–9). Figures 4–9 give a clearer picture of the interactive effects of any two of the parameters while the others were constant.

Binary Effect of Initial *p*-NA Concentration and pH

The binary effect of the initial *p*-NA concentration and pH of the solution on the amount of *p*-NA removed by TiO_2-FSAC is given in Figure 4. The experiment was carried out at a fixed time of 362.5 min and a TiO_2-FSAC dosage of 0.10 g. Figure 4 shows that increasing the *p*-NA initial concentration at lower pH increases the amount of *p*-NA removal per gram. The increase in the amount of *p*-NA removed as the initial *p*-NA concentration increases is due to increased concentration of *p*-NA ions in the solution. At low pH, the uptake of *p*-NA was at maximum. This is because there are more positive ammonium ions in the solution. Hence, the rise in the quantity of *p*-NA removal at lower pH is due to the electrostatic attraction between the protonated species of *p*-NA in the solution and the surface of TiO_2-FSAC. Indeed, at higher pH, the removal of *p*-NA becomes unfavorable[4,24].

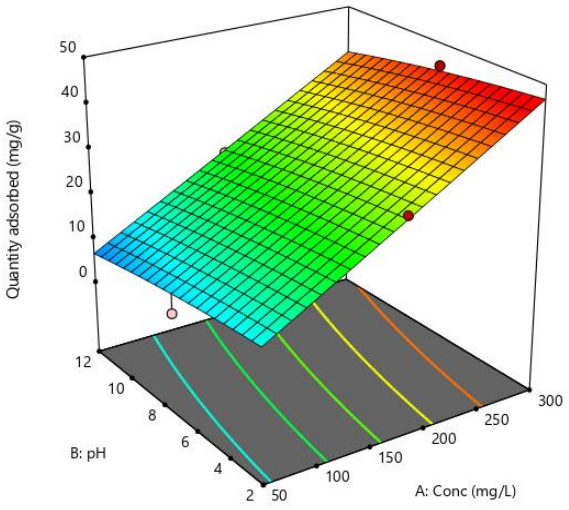


Figure 4. 3D response surface plot of the binary effect of initial concentration and pH at a fixed 0.10 g dosage and 362.5 min contact time on the quantity of *p*-NA adsorbed onto TiO_2-FSAC.

Binary Effect of Initial *p*-NA Concentration and Dosage

Figure 5 represents the binary effect of initial *p*-NA concentration and adsorbent dosage on the amount of *p*-NA removal per gram by TiO_2-FSAC at a constant contact time of 362.5 min and pH 2. These are the only significant interaction terms in establishing the highest amount of *p*-NA removed by TiO_2-FSAC. The increase in initial *p*-NA concentration immensely affects the adsorption of *p*-NA onto TiO_2-FSAC. However, the uptake of *p*-NA onto TiO_2-FSAC was at maximum at low adsorbent dosage. The rapid adsorption of *p*-NA experienced at lower dosage is ascribed to the availability of many free adsorption sites on the adsorbent surface. At high dosage, adsorbed *p*-NA will be distributed over a larger amount of the adsorbent, leading to lower quantity of *p*-NA adsorbed per gram (mg/g)[4,25].

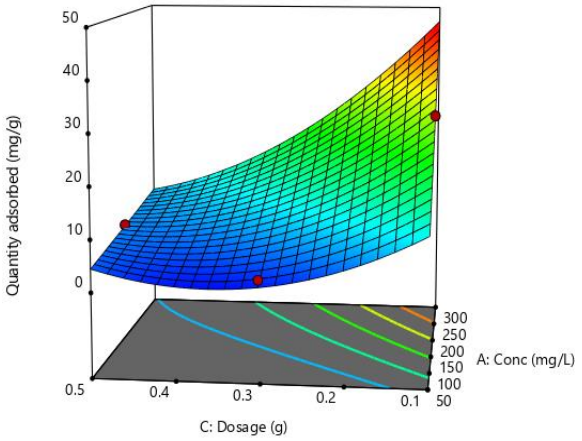


Figure 5. 3D response surface plot of the binary effect of initial *p*-NA concentration and dosage at fixed pH 2 and 362.5-min contact time on the amount of *p*-NA adsorbed onto TiO_2-FSAC.

Binary Effect of Initial *p*-NA Concentration and Contact Time

Figure 6 reveals the interactive effect between initial *p*-NA concentration and contact time on the response surface for the quantity of *p*-NA uptake by TiO_2-FSAC at constant pH and adsorbent dosage. The combined effect of these factors shows no significant influence on the amount of *p*-NA removed by TiO_2-FSAC, as seen in Table 4. It can be deduced that the amount of *p*-NA uptake is enhanced with increased initial *p*-NA concentration in the solution. An increase in contact time has little effect on the amount of *p*-NA removed. This is because there are abundant vacant sites initially ready for adsorption at the beginning of the process. As adsorption progresses, *p*-NA molecules fill more vacant sites on the adsorbent surface, but in general, equilibrium is established quickly, which is the reason why there was no major difference in the quantity of *p*-NA adsorbed over the time range investigated.

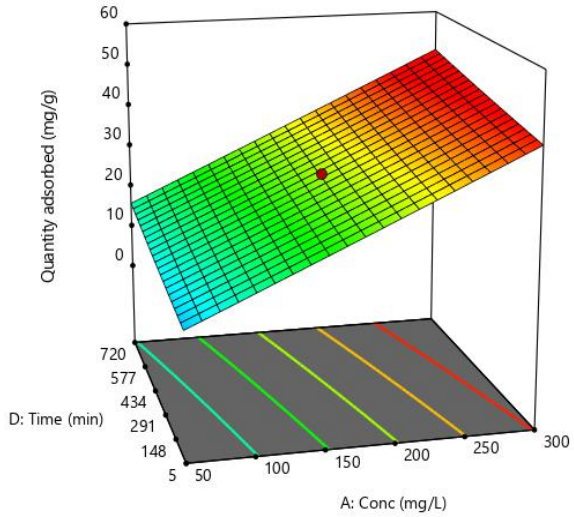


Figure 6. 3D response surface plot of the binary effect of initial *p*-NA concentration and Contact time at fixed pH 2 and 0.10 g/20 mL adsorbent dosage on the quantity of *p*-NA adsorbed onto TiO_2-FSAC.

Binary Effect of pH and Contact Time

Figure 7 depicts the binary effect of pH and contact time on the response of *p*-NA removal from the aqueous solution at a fixed initial *p*-NA concentration and TiO_2-FSAC dosage. The binary effect is not significant (Table 4), but the non-significance of these factors, when considered together, was used as justification for achieving the optimum conditions for this study. This figure gives the center point values of 2 and 362.5 min for pH and contact time, respectively, which was utilized with the other parameters to get the optimum conditions essential to efficiently remove *p*-NA from the aqueous solution by TiO_2-FSAC. This figure gave the optimum actual and predicted removal of *p*-NA values of 45.02 mg/g and 43.90 mg/g, respectively, at the center point values of 300 mg/L initial *p*-NA concentration, pH 2, 362.5 min and 0.10 g adsorbent dosage. A further increase in pH and time will result in a reduction in the amount of *p*-NA adsorbed[26,27].

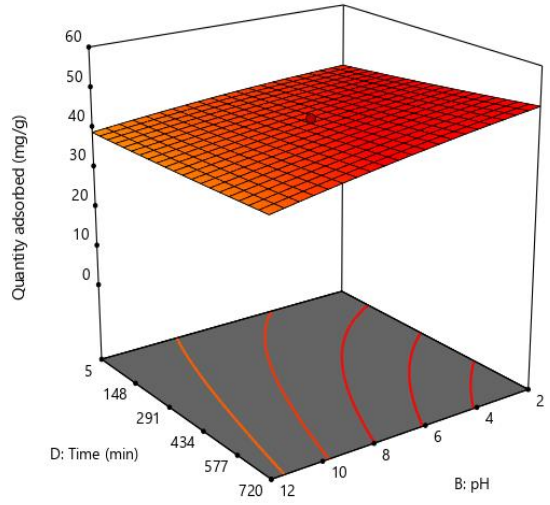


Figure 7. 3D response surface plot of the binary effect of pH and contact time at a fixed 300 mg/L initial *p*-NA concentration and 0.10 g adsorbent dosage on the quantity of *p*-NA adsorbed onto TiO_2-FSAC.

Binary Effect of pH and Dosage

Figure 8 represents the influence of the interaction between pH and dosage on the response surface for *p*-NA removal from the aqueous solution at constant initial *p*-NA concentration and contact time. The adsorption of *p*-NA is favorable at low pH and low dosage, indicating a synergistic interaction between these two factors.

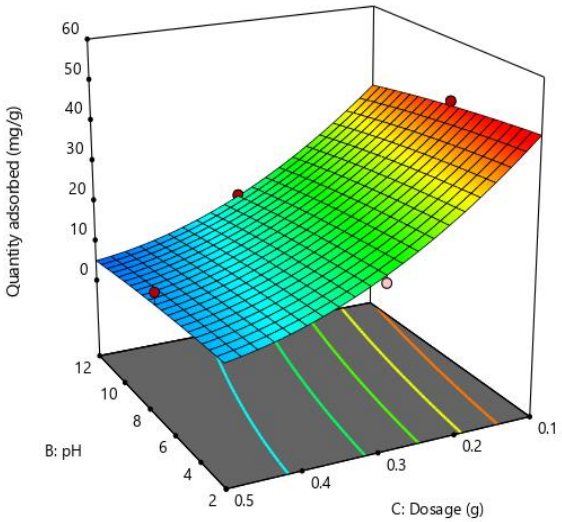


Figure 8. 3D response surface plot of the binary effect of pH and adsorbent dosage at a fixed 300 mg/L-initial *p*-NA concentration and 362.5-min contact time on the quantity of *p*-NA adsorbed onto TiO_2-FSAC.

Binary Effect of Contact Time and Dosage

The simultaneous effect of contact time and dosage on the response surface for the amount of *p*-NA uptake by TiO_2-FSAC at constant pH and initial *p*-NA concentration is presented in Figure 9. These two parameters have an antagonistic effect on the quantity of *p*-NA removed by TiO_2-FSAC[28]. It can be seen that the quantity of *p*-NA adsorbed is at the highest at a low dosage of 0.10 g TiO_2-FSAC and very rapid at the begin of the process. This is due to the availability of numerous vacant sites ready for adsorption in the early stage of the process. However, an increase in contact time and adsorbent dosage decreases the quantity of *p*-NA removal, primarily due to increased dosage reflecting the distribution of *p*-NA over a larger amount of adsorbent.

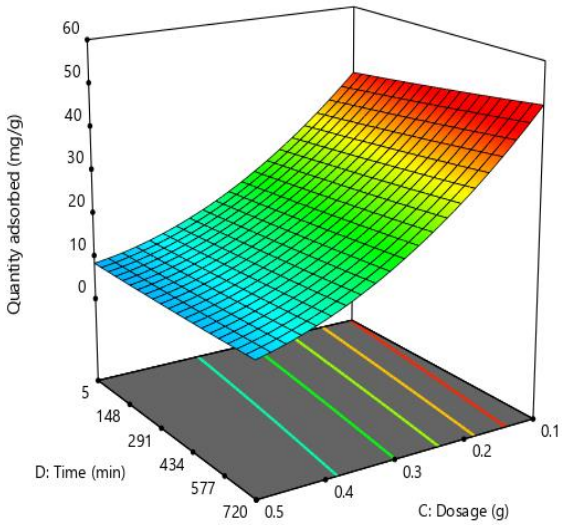


Figure 9. 3D response surface plot of the binary effect of contact time and dosage at a fixed 300 mg/L initial *p*-NA concentration and pH 2 on the quantity of *p*-NA adsorbed onto TiO_2-FSAC.

Table 5 shows the comparison of the adsorption efficiency between TiO_2-FSAC and bear FSAC under optimized conditions. The quantity of *p*-NA adsorbed by TiO_2-FSAC is greater than that adsorbed by FSAC. The enhanced adsorption removal of TiO_2-FSAC could be due to the presence of TiO_2 particles in the adsorbent.

Table 5. Comparison of adsorption efficiencies of TiO_2-FSAC and FSAC under optimized conditions for *p*-NA removal.

Optimum conditions				Response (mg/g)	
Concentration (mg/L)	pH	Dosage (g)	Time (min)	TiO_2-FSAC	FSAC
300	2	0.10	362.5	45.02	40.04

Interactive Effects of the Process Parameters

The perturbation plot is largely used to determine the influence of individual parameters on the response. The response is designed by altering one parameter only while keeping other factors unchanged at the center of the plot. Therefore, a perturbation plot is a design used in knowing the parameter that most affects the adsorption process. Figure 10 shows that adsorbent dosage has the most significant effects on the amount of *p*-NA adsorbed by TiO_2-FSAC due to its curvature compared to other parameters with relative linearity. This is similar to the report of Oghenejoboh[25].

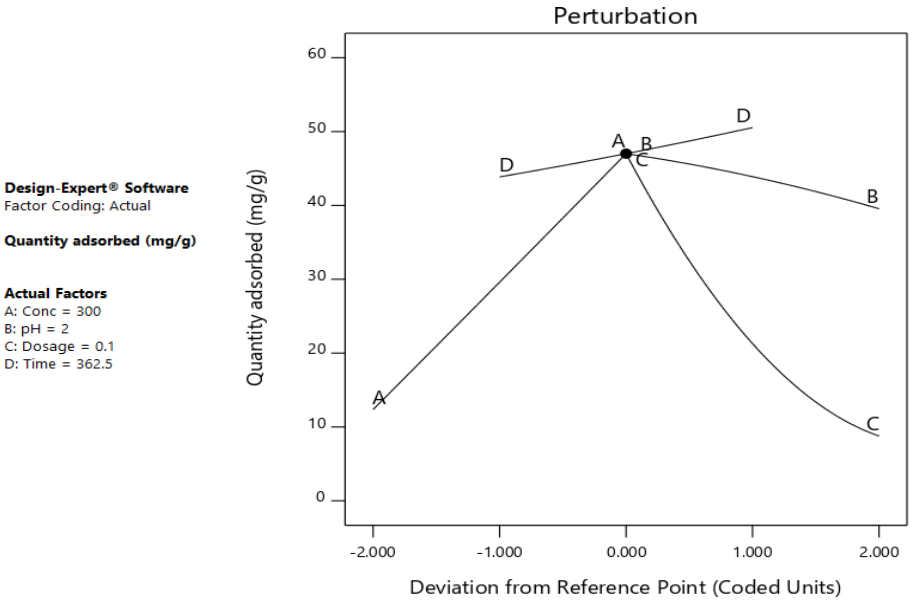


Figure 10. Perturbation plots for the amount of *p*-NA adsorbed by TiO_2-FSAC.

Percentage Contribution of Process Parameters on the Response Surface plots

The percentage contribution (%C) of each parameter on the response model was studied by Equation 6[27,29]:

$$\%C = \frac{SS_i}{SS_m} \times 100 \qquad (6)$$

where SS_m is the sum of squares for the model and SS_i is the sum of squares for the individual parameters. Table 4 presents the results and indicates that the adsorbent dosage, initial *p*-NA concentration and pH of the solution contributed enormously to *p*-NA adsorption by TiO_2-FSAC. The %C of contact time is the lowest among the individual parameters in the response model. The interactive term AC has a %C value of 7.68 and the quadratic term C^2 has a %C value of 9.38, while the other terms have lower contributions in *p*-NA adsorption from the aqueous solution.

Conclusion

This research shows that flamboyant seeds-activated carbon-titanium(IV) oxide composite is a potential and effective adsorbent for *p*-NA removal from aqueous media. The Box-Behnken design under response surface methodology (BBD-RSM) was successfully utilized to establish the optimum conditions for the adsorption process. The results showed that the quantity of *p*-NA adsorbed increased with an increase in initial *p*-NA concentration, low pH and adsorbent dosage and was not affected by contact time. The correlation between *p*-NA adsorption by TiO_2-FSAC and the operating parameters was adequately developed by the

quadratic model with high regression coefficient (R^2 = 0.973), which agrees with the adjusted one (R^2 = 0945). The optimum condition for *p*-NA adsorption was found to be 300 mg/L-initial *p*-NA concentration, pH 2, 362.5-min contact time and 0.10 g adsorbent dosage, relating to 45.02 mg/g actual removal in agreement with predicted removal of 43.90 mg/g. It was also established that initial *p*-NA concentration, pH of the solution, adsorbent dosage and interaction between initial *p*-NA concentration and adsorbent dosage significantly influenced the adsorption of *p*-NA from aqueous media, while contact time in the investigated range did not significantly affect the process.

Acknowledgments

This work was supported by the Kwara State University, Department of Chemistry and Industrial Chemistry, Faculty of Pure and Applied Sciences, Malete. Nigeria.

References

[1] Zheng, K.; Pan, B.; Zhang, Q.; Zhang, W.; Pan, B.; Han, Y.; Zhang. Q.; Wei, D.; Xua, Z.; Zhang, Q., *Sep. Purif. Technol.*, **2007**, *57*, 250–56.

[2] Sun, J. H.; Sun, S. P.; Fan, M. H.; Guo, H. Q.; Lee, Y.F. ; Sun, R. X., *J. Hazard Mater.*, **2008**, *153*, 187–193.

[3] Li, K.; Li, Y.; Zheng, Z., *J. Hazard Mater.*, **2010**, *178*, 553–559.

[4] Azeez S. O.; Adekola, F. A., *Jordan J. Chem.*, **2016**, *11*, 128–145.

[5] Malakootian M.; Pournamdari, M.; Asadipour, A. ; Mahdizadeh, H., *Korean J. Chem. Eng.*, **2019**, *36*, 217–225.

[6] Amuda, O. S.; Olayiwola, A. O.; Alade, A. O., *J. Environ. Prot.*, **2014**, *5*, 1352–1363.

[7] Ghorbani, F.; Kamari, S., *Adsorpt. Sci. Technol.*, **2017**, *35*, 317–338.

[8] Al-Bayati, T. M., *Part. Sci. Technol.*, **2014**, *32*, 616–623.

[9] El-Safty, S. A.; Ismael. M.; Shahat A.; Shenashen M. A., *Environ. Sci. Pollut. Res.*, **2013**, *20*, 3863–3876.

[10] Orha, C.; Lazau C.; Ursu, D.; Manea F., *Water Soc. IV*, **2017**, *216*, 230–211.

[11] Azhar, Z.; Ramli, R. M.; Noorfidza Y. H., *Technologies*, **2017**, *5*, 1–13.

[12] Rezaee, A.; Pourtaghi, G. H.; Khavanin, A.; Mamoory, R. S.; Ghaneian, M. T.; Godini, H., *Iran J. Environ. Heal. Sci. Eng.*, **2008**, *5*, 305–310.

[13] Lib, I.; Webb, D. B.; Wood, P. J., *A Guide to Species Selection for Tropical and Sub-tropical Plantations*, Second Edition, University of Oxford, 1984, pp 1–255.

[14] Anfar, Z.; Ahsaine, H.; Zbair, M.; Amedlous, A.; El Fakir, A. A.; Jada, A.; El Alem, N., *Crit. Rev. Environ. Sci. Technol.*, **2020**, *50*, 1043–1084.

[15] Peng, X.; Yang, G.; Shi, Y.; Zhou, Y.; Zhang, M.; Li, S., *Sci. Rep.*, **2020**, *10*, 1–10.

[16] Brahmi, L.; Kaouah, F.; Bourmaza, S.; Trari, M., *Appl. Water Sci.*, **2019**, *9*, 1–13.

[17] Kibanova, D.; Trejo, M. ; Destaillats, H.; Cervini S., *Appl. Clay Sci.*, **2009**, *42*, 563–568.

[18] Zawawi, A.; Ramli, R. M.; Harunl, N. Y., *Malaysian J. Anal. Sci.*, **2018**, *22*, 648–658.

[19] Saheed, I. O.; Adekola, F. A.; Olatunji, G. A., *J. Turkish Chem. Soc.-Sect. A, Chem.*, **2016**, *4*, 375–395.

[20] Penas-garz, M.; Almudena, G.; Bedia, J.; Rodriguez, J. J.; Belver, C., *Materials*, **2019**, *12*, 1–17.

[21] Arana, J.; Rendon, E. T.; Garriga, C.; Herrera-Melian, J. A.; Perez-pena, J.; Colon, G.; Navio, J. A., *Appl. Catal. B, Environ.*, **2003**, *44*, 153–160.

[22] Zeitler, V. A.; Brown, C. A., *J. Phys. Chem.*, **1957**, *61*, 1174–1177.

[23] Alman-Abad, Z. S.; Pirkharrati, H.; Asadzadeh, F.; Maleki-Kakelar, M., *Adsorpt. Sci. Technol.*, **2020**, *38*, 79–93.

[24] Ben Khalifa, E.; Rzig, B.; Chakroun, R.; Nouagui, H.; Hamrouni, B., *Chemom. Intell. Lab Syst.*, **2019**, *189*, 18–26.

[25] Oghenejoboh, K. M., *Nigerian J. Technol.*, **2018**, *37*, 647–655.

[26] Allouss, D.; Essamlali, Y.; Amadine, O.; Chakir, A.; Zahouily, M., *RSC Adv.*, **2019**, *9*, 37858–37869.

[27] Rahman, N.; Nasir, M., *Environ. Sci, Pollut. Res.*, **2018**, *25*, 26114–26134.

[28] Azeez, S. O.; Saheed, I. O.; Adekola, F. A.; Jimoh, A. A.; Aransiola, D. M.; Abdulsalam, Z. A., *J. Turkish Chem. Soc.-Sect. A, Chem.*, **2022**, *9*, 205–222.

[29] Bandari, F.; Safa, F.; Shariati, S., *Arab J. Sci. Eng.*, **2015**, *40*, 3363–3372.